

# Temperatures and metallicities of M giants in the galactic Bulge from low-resolution K-band spectra <sup>★</sup>

M. Schultheis<sup>1</sup>, N. Ryde<sup>2</sup>, and G. Nandakumar<sup>1</sup>

<sup>1</sup> Laboratoire Lagrange, Université Côte d'Azur, Observatoire de la Côte d'Azur, CNRS, Blvd de l'Observatoire, F-06304 Nice, France e-mail: mathias.schultheis@oca.eu

<sup>2</sup> Department of Astronomy and Theoretical Physics, Lund Observatory, Lund University, Box 43, 221 00, Lund, Sweden e-mail: ryde@astro.lu.se

January 3, 2018

## ABSTRACT

**Context.** With the existing and upcoming large multi-fibre low-resolution spectrographs, the question arises how precise stellar parameters such as  $T_{\text{eff}}$  and  $[\text{Fe}/\text{H}]$  can be obtained from low-resolution K-band spectra with respect to traditional photometric temperature measurements. Until now, most of the effective temperatures in galactic Bulge studies come directly from photometric techniques. Uncertainties in interstellar reddening and in the assumed extinction law could lead to large systematic errors ( $> 200$  K).

**Aims.** We aim to obtain and calibrate the relation between  $T_{\text{eff}}$  and the  $^{12}\text{CO}$  first overtone bands for M giants in the galactic Bulge covering a wide range in metallicity.

**Methods.** We use low-resolution spectra for 20 M giants with well-studied parameters from photometric measurements covering the temperature range  $3200 < T_{\text{eff}} < 4500$  K and a metallicity range from 0.5 dex down to -1.2 dex and study the behaviour of  $T_{\text{eff}}$  and  $[\text{Fe}/\text{H}]$  on the spectral indices.

**Results.** We find a tight relation between  $T_{\text{eff}}$  and the  $^{12}\text{CO}(2 - 0)$  band with a dispersion of 95 K as well as between  $T_{\text{eff}}$  and the  $^{12}\text{CO}(3 - 1)$  with a dispersion of 120 K. We do not find any dependence of these relations on the metallicity of the star, making them relation attractive for galactic Bulge studies. This relation is also not sensitive to the spectral resolution allowing to apply this relation in a more general way. We also found a correlation between the combination of the NaI, CaI and the  $^{12}\text{CO}$  band with the metallicity of the star. However this relation is only valid for sub-solar metallicities.

**Conclusions.** We show that low-resolution spectra provide a powerful tool to obtain effective temperatures of M giants. We show that this relation does not depend on the metallicity of the star within the investigated range and is also applicable to different spectral resolution making this relation in general useable to derive effective temperatures in high extinguished regions where photometric temperatures are not reliable.

**Key words.** Galaxy: bulge, structure, stellar content – stars: fundamental parameters: abundances -infrared: stars

## 1. Introduction

While photometric temperatures can be estimated quite precisely in low-extinction windows (see e.g. González Hernández & Bonifacio 2009), regions where interstellar reddening is high (e.g. galactic Bulge, galactic plane), photometric temperatures, by definition, suffer from large and unknown systematic uncertainties. Going even closer to the Galactic Centre region ( $R_{\text{GC}} < 200$  pc) it is virtually impossible to get reliable photometric temperatures due to the extreme high interstellar reddening (Schultheis et al. 2009, Gonzalez et al. 2012, Schultheis et al. 2014). To overcome this problems, Ryde & Schultheis (2015), for example, instead derived  $T_{\text{eff}}$  from spectral indices in low-resolution K band spectra in their study of Galactic center stars. They were then able to obtain accurate detailed chemical abundances of nine M giant stars close to the Galactic Center using the CRIFES high-resolution spectrograph. This technique was extended to latitudes at  $b = -1^\circ$  and  $b = -2^\circ$  (Ryde et al. 2016).

Ramirez et al. (1997) and Ramirez et al. (2000) studied the behaviour of the  $^{12}\text{CO}$  band head situated at  $2.3 \mu\text{m}$  with low-resolution K-band spectra ( $R \sim 2000 - 4000$ ) and found for M

giants a remarkably tight relation between the equivalent width (EW) and the effective temperature. Blum et al. (2003) and Ivanov et al. (2004) confirmed this strong temperature dependence of the  $^{12}\text{CO}$  band head using different spectral resolution.

Ramírez et al. (2000), Frogel et al. (2001), Schultheis et al. (2003) and Ivanov et al. (2004) found that the combined index of the NaI doublet at  $2.21 \mu\text{m}$  and the CaI triplet at  $2.261 \mu\text{m}$  is very sensitive to the surface gravity of the star and can be used to separate, e.g., M giants from supergiants or dwarf stars. Schultheis et al. (2003) has shown the power of low-resolution spectra in the region of high interstellar extinction. They could separate different stellar populations such as red giant branch stars, AGB stars, supergiants or young stellar objects. Frogel et al. (2001) and Ramírez et al. (2000) obtained relations between  $\text{EW}(\text{NaI})$ ,  $\text{EW}(\text{CaI})$  and  $[\text{Fe}/\text{H}]$  which were calibrated on globular clusters. Based on this calibration, Ramírez et al. (2000) studied the metallicity distributions in the Galactic center region and found no evidence of a metallicity gradient for the Inner Bulge. Pfuhl et al. (2011) determined the average star formation rate from 450 cool giant stars located in the nuclear star cluster. They obtained low-resolution spectra ( $R \sim 2000 - 3000$ ) of 33 giants in the solar neighbourhood ( $-0.3 < [\text{Fe}/\text{H}] < 0.2$ ) with spectral types from G0–M7 and obtained a  $\text{CO} - T_{\text{eff}}$  relation with a residual

<sup>★</sup> Based on observations collected at the European Southern Observatory, Chile, program number 089.B-0312B

scatter of 119 K. However, the  $T_{\text{eff}}$  vs.  $^{12}\text{CO}$  calibration has been only investigated for a bright local solar-neighbourhood sample with a narrow metallicity range. We extend this study for M giants located in the galactic Bulge using a wide metallicity range to test this calibration.

Until now most of the abundance studies (e.g. Rich & Origlia 2012, Gonzalez et al. 2011, Zoccali et al. 2008) in galactic Bulge fields use photometric temperatures based on a colour-temperature relation and assuming interstellar reddening values **as a first temperature estimate**. However, variable extinction, uncertainties in the extinction law, etc. can lead to severe uncertainties in the derived temperatures ( $> 200$  K) which can lead to unknown and different systematic offsets, in the abundance determination. Here we apply and investigate these relations for stellar abundances studies in the Bulge, extending their use for a wide range of metallicities

In this paper, we show how low-resolution spectra can provide a powerful tool to get high accurate effective temperatures in highly extinguished regions (such as the Galactic Center). We are able to show that this method chosen by, e.g. Ryde & Schultheis (2015) and Ryde et al. (2016), indeed is a good choice. The paper is structured as following: In Sect. 2 we describe the data and the data reduction process, in Sect. 3 we discuss how the known effective temperature, and metallicity of our calibration stars relates with the CO bands and the spectral indices such as NaI and CaI, in Sect. 4 we apply our method to M giants in the inner Galactic bulge and we finish in Sect. 5 with the conclusions.

## 2. Observations

We obtained near-IR spectra on 27 June – 30 June 2010 with ISAAC at ESO, Paranal, Chile. We used the red grism of the ISAAC spectrograph, covering 2.0–2.53  $\mu\text{m}$ , to observe 21 M giants in the galactic Bulge. We took the spectra under photometric conditions through a 1'' slit providing a resolving power of  $R \sim 2000$ . We obtained a Ks-band acquisition image before each spectrum to identify the source and place it on the slit. We used UKIDSS finding charts for source identification and to choose “empty” sky positions for sky subtraction for each source along the 90'' slit. We used an “ABBA” observing sequence for optimal sky subtraction.

We observed B dwarfs (typically 6-8 stars per night), close to the airmass range of our targets, as telluric standard stars to correct for the instrumental and atmospheric transmission. We used IRAF to reduce the ISAAC spectra. We removed cosmic ray events, subtracted the bias level, and then divided all frames by a normalized flat-field. We used the traces of stars at two different (AB) positions along the slit to subtract the sky. After extracting and co-adding the spectra, we calibrated wavelengths using the Xe-lamp. The r.m.s. of the wavelength calibration is better than 0.5  $\text{\AA}$ .

We rebinned the spectra to a linear scale, with a dispersion of  $\sim 7 \text{\AA}$  pixel and a wavelength range from 2.0  $\mu\text{m}$  to 2.51  $\mu\text{m}$ . We then divided each spectrum by the telluric standard observed closest in time and in airmass (airmass difference  $< 0.05$ ). We then normalized the resulting spectra by the mean flux between 2.27 and 2.29  $\mu\text{m}$ . Table 1 shows the list of known Bulge stars with precise stellar parameters. Our stars lie in the temperature range  $3200 < T_{\text{eff}} < 4500$  K and are selected from Rich & Origlia (2005), Rich et al. (2012), Gonzalez et al. (2011a) and Monaco et al. (2011). They span a wide range in metallicities ensuring that we can study an eventual metallicity dependence of the CO vs.  $T_{\text{eff}}$  relation

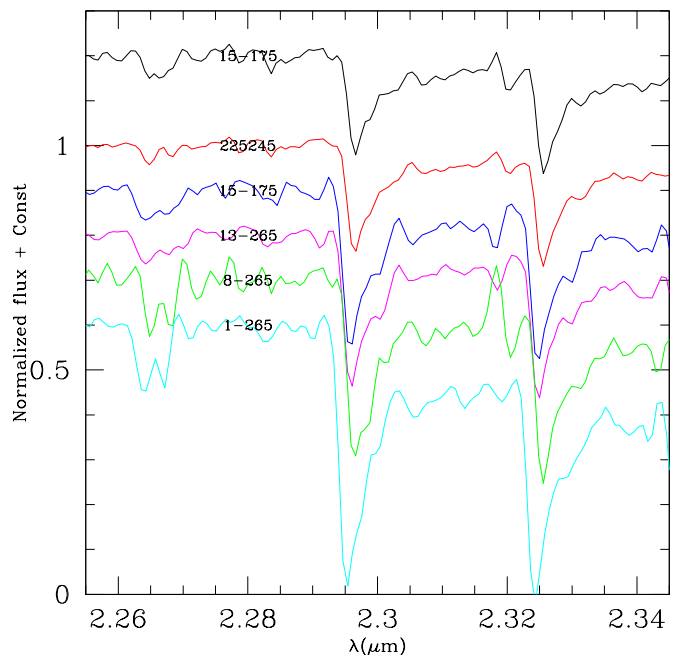


**Fig. 1.** Temperature sequence of the CO bandhead starting from 4500 K (black) going down to 3200 K (cyan) in 200 K steps. Indicated are the star names (see Table. 1).

Figure 1 shows the temperature sensitivity of the CO bandhead where we see a steady increase of the absorption band with effective temperature.

### 2.1. Stellar samples: calibrators and target M giants

Our sample of stars cover M giants sample in Baade’s window from Rich & Origlia (2005) and Gonzalez et al. (2011b). All are from low extinction fields where we can trust and account for the reddening in an accurate way. In addition, we include stars of Rich et al. (2012) which are located at  $l = 0^\circ$  and  $b = -1^\circ$ . This field which is close to the Galactic Center shows well studied interstellar extinction (see e.g. Schultheis et al. 1999, Gonzalez et al. (2012), etc.). The other stars come from the thick disc study of Monaco et al. (2011) where the temperatures were obtained by using the dereddened  $(J - K)_0$  colour but with small and well quantified reddening.

We will use our derived calibration based on the stars in Table 1, on a sample of stars in the highly extinguished inner bulge region. Thus, we have also observed, with the same instrument setup 28 Bulge M giants within 2 degrees from the Galactic Center, along the Southern minor axis to obtain effective temperatures. These 28 stars were also observed with CRIRES in order to get detailed chemical abundances (see Ryde & Schultheis 2015, Ryde et al. 2016). 9 stars were observed in the Galactic Center (Ryde & Schultheis 2015), 9 stars at  $(l, b) = (0, -1^\circ)$ , and 10 stars at  $(l, b) = (0, -2^\circ)$ . These stars are M giants with  $T_{\text{eff}} = 3300\text{--}4200$  K and  $0.7 < \log g < 2.25$ , for which metallicities,  $[\text{Fe}/\text{H}]$ , and the abundances of the  $\alpha$  elements Mg, Si, and Ca were determined. Table 2 shows the M giant sample of Ryde et al. (2016) together with the derived effective temperatures and metallicities in this work (see Sect. 4) and the metallicities derived in Ryde et al. (2016).

**Table 1.** List of observed targets together with ra, dec, K magnitude, spectral type,  $T_{\text{eff}}$ ,  $\log g$  and  $[\text{Fe}/\text{H}]$ .

| name                   | ra          | dec         | K     | Sptype | Teff | log g | [Fe/H] |
|------------------------|-------------|-------------|-------|--------|------|-------|--------|
| BMB28 <sup>1</sup>     | 18:02:59.51 | -30:02:54.3 | 7.39  | M7     | 3400 | 0.5   | -0.22  |
| BMB55 <sup>1</sup>     | 18:03:08.11 | -29:57:48.0 | 7.78  | M8     | 3200 | 0.5   | -0.17  |
| BMB93 <sup>1</sup>     | 18:03:22.34 | -30:02:56.4 | 7.28  | M6     | 3600 | 0.5   | -0.15  |
| BMB124 <sup>1</sup>    | 18:03:29.72 | -29:55:57.6 | 8.84  | M6     | 3600 | 0.5   | -0.15  |
| BMB152 <sup>1</sup>    | 18:03:36.92 | -30:01:47.4 | 7.31  | M9     | 3200 | 0.5   | -0.24  |
| BMB165 <sup>1</sup>    | 18:03:43.78 | 30:05:17.2  | 8.10  | M7     | 3400 | 0.5   | -0.29  |
| BMB289 <sup>1</sup>    | 18:04:22.66 | -29:54:51.8 | 6.20  | M9     | 3200 | 0.5   | -0.15  |
| 1-265 <sup>2</sup>     | 17:58:37.12 | -29:03:48.4 | 8.34  | M9     | 3200 | –     | -0.08  |
| 8-265 <sup>2</sup>     | 17:58:43.83 | -29:07:42.5 | 8.23  | M7     | 3400 | –     | -0.19  |
| 13-265 <sup>2</sup>    | 17:58:37.41 | -28:59:33.2 | 8.32  | M6     | 3600 | –     | -0.36  |
| 142173 <sup>4</sup>    | 00:32:12.56 | -38:34:02.3 | 9.29  | –      | 4330 | 1.50  | -0.69  |
| 15-175 <sup>2</sup>    | 17:52:53.33 | -29:58:49.8 | 8.90  | M5     | 3800 | –     | -0.37  |
| 171877 <sup>4</sup>    | 00:39:20.23 | -31:31:35.5 | 8.12  | –      | 3930 | 1.10  | -0.77  |
| 225245 <sup>4</sup>    | 00:54:46.38 | -27:35:30.4 | 8.79  | –      | 3920 | 0.65  | -0.99  |
| 313132 <sup>4</sup>    | 01:20:20.66 | -34:09:54.1 | 7.04  | –      | 4530 | 2.0   | 0.01   |
| 343555 <sup>4</sup>    | 01:29:42.01 | -30:15:46.4 | 8.46  | –      | 4530 | 2.25  | -0.62  |
| 42 <sup>3</sup>        | 18:10:17.65 | -31:45:38.9 | 8.81  | –      | 3750 | 1.20  | -0.96  |
| 6 <sup>3</sup>         | 18:09:59.53 | -31:38:14.1 | 12.08 | –      | 3900 | 1.47  | 0.20   |
| 86 <sup>3</sup>        | 18:35:15.24 | -34:46:41.4 | 12.41 | –      | 3850 | 1.66  | 0.42   |
| BD-012971 <sup>1</sup> | 14:38:48.04 | -02:17:11.5 | 4.3   | M5     | 3600 | 0.5   | -0.78  |

<sup>1</sup> Rich & Origlia (2005)

<sup>2</sup> Rich et al. (2012)

<sup>3</sup> Gonzalez et al. (2011)

<sup>4</sup> Monaco et al. (2011)

**Table 2.** Effective temperatures from this work, metallicities from the high resolution work of Ryde et al. (2016), and metallicities from this work (third column) of the galactic Bulge M giant sample.

| Star   | $T_{\text{eff}}$ | $[\text{Fe}/\text{H}]_{\text{CRILES}}$ | $[\text{Fe}/\text{H}]_{\text{low}}$ |
|--------|------------------|--|-------------------------------------|
| GC1    | 3667             | 0.15                                   | -0.15                               |
| GC20   | 3684             | 0.14                                   | -0.05                               |
| GC22   | 3614             | 0.04                                   | -0.02                               |
| GC25   | 3648             | -0.20                                  | 0.07                                |
| GC27   | 3405             | 0.23                                   | 0.19                                |
| GC28   | 3736             | -0.04                                  | -0.30                               |
| GC29   | 3420             | 0.12                                   | -0.31                               |
| GC37   | 3747             | -0.08                                  | 0.19                                |
| GC44   | 3461             | 0.18                                   | 0.24                                |
| bm1-06 | 3764             | 0.29                                   | -0.1                                |
| bm1-07 | 3863             | 0.08                                   | -0.23                               |
| bm1-08 | 3618             | 0.17                                   | -0.25                               |
| bm1-10 | 3762             | -0.23                                  | -0.45                               |
| bm1-11 | 3734             | 0.12                                   | -0.14                               |
| bm1-13 | 3717             | -0.94                                  | -0.53                               |
| bm1-17 | 3770             | -0.83                                  | -0.844                              |
| bm1-18 | 3781             | 0.22                                   | -0.28                               |
| bm1-19 | 3905             | 0.18                                   | -0.17                               |
| bm2-01 | 3948             | 0.14                                   | -0.62                               |
| bm2-02 | 3990             | -0.48                                  | -0.60                               |
| bm2-03 | 3666             | 0.26                                   | -0.34                               |
| bm2-05 | 3451             | 0.01                                   | -0.04                               |
| bm2-06 | 4172             | -1.17                                  | -1.23                               |
| bm2-11 | 3961             | -0.91                                  | -0.85                               |
| bm2-12 | 3943             | -0.11                                  | -0.28                               |
| bm2-13 | 3746             | -0.16                                  | -0.42                               |
| bm2-15 | 3984             | 0.22                                   | -0.13                               |
| bm2-16 | 3838             | 0.10                                   | -0.16                               |

**Table 3.** Band passes and continuum points of the  $^{12}\text{CO}$  bands.

| Feature                         | $\lambda_c$ (Å) | $\Delta\lambda$ (Å) |
|---------------------------------|-----------------|---------------------|
| $^{12}\text{CO}(2-0)$           | 23020           | 150                 |
| $^{12}\text{CO}(2-0)$ continuum | 22840           | 150                 |
| $^{12}\text{CO}(3-1)$           | 23245           | 54                  |
| $^{12}\text{CO}(3-1)$ continuum | 22840           | 150                 |

### 3. The method: empirical temperatures and metallicities

We discuss in this Sect. our method based on our calibration sample (Table. 1).

#### 3.1. Effective temperature

When measuring the equivalent width of the  $^{12}\text{CO}$  band, the choice of the pseudo-continuum bands is important (see e.g. Ivanov et al. (2004)). We have tested different continuum bands such as Ramírez et al. (2000), Frogel et al. (2001), Ivanov et al. (2004), Pfuhl et al. (2011) and looked for the smallest dispersion in  $T_{\text{eff}}$  in our sample. We have found that the Blum et al. (2003) bandpasses and continuum points show in general the smallest r.m.s dispersion. The absorption indices defined by Blum et al. (2003) are measured relative to spectral regions adjacent to the absorption itself and are thus independent of reddening. The  $^{12}\text{CO}(2-0)$  index is defined as the percentage of the flux in the  $^{12}\text{CO}(2-0)$  feature relative to a continuum band centered at  $2.284\ \mu\text{m}$ . The  $^{12}\text{CO}(2-0)$  band and continuum band is  $0.015\ \mu\text{m}$  wide and the  $^{12}\text{CO}(2-0)$  band is centered at  $2.302\ \mu\text{m}$  (see Blum et al. 2003). In addition, we also measure the  $^{12}\text{CO}(3-1)$  bandhead. Table 1 gives central wavelengths and bandpasses for the CO lines and their pseudo-continuum.

Figure 2 shows the  $^{12}\text{CO}(2-0)$  index of the Blum et al. (2003) sample as well as our sample. The black lines give the fitted relation of Blum et al. (2003) with  $T_{\text{eff}} = 4828.0 - 77.5 \times \text{CO}(2-0)$  which is very similar to our linear least-square fit. The r.m.s of the fit is 95 K which is comparable with the r.m.s scatter of Pfuhl et al. (2011).

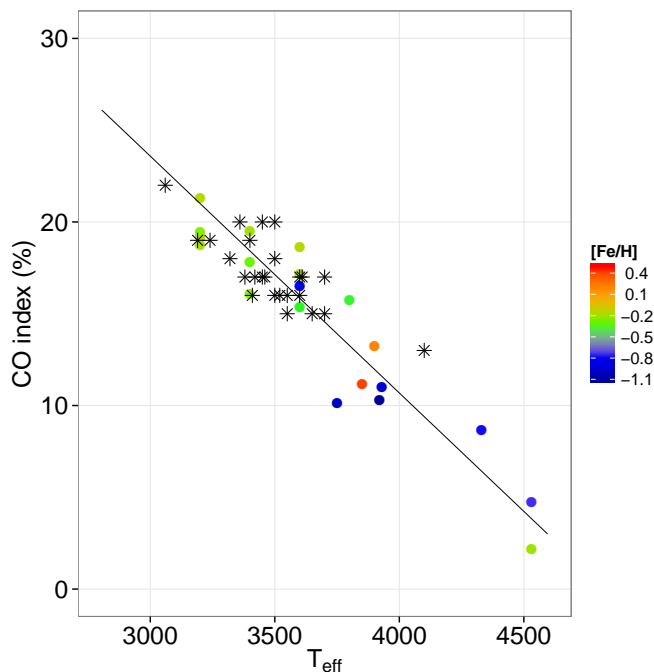


**Fig. 2.** Effective temperature vs.  $^{12}\text{CO}(2-0)$  band as a function of metallicity. Black asterisks are the stars from Blum et al. (2003) The straight line shows the fitted relation by Blum et al. (2003).

The Blum et al. (2003) sample covers bright solar neighbourhood giant stars (see their Table.3) with typical solar metallicities. We extended this work for galactic Bulge stars in low extinction fields covering a wide metallicity range with  $-1.2 < [\text{Fe}/\text{H}] < 0.5$  which enables to test any possible metallicity dependence of this relation. As shown in Fig. 2, we do not find any metallicity dependence on this relation within the metallicity range of our calibration stars, relevant for the bulge, making this method extremely interesting for galactic Bulge studies. The spectral resolution of the comparison stars in Blum et al. (2003) is  $\sim 750$ . As one sees in Fig. 2 the effect of using a different instrument setup with a different spectral resolution (i.e.  $R \sim 2000$  vs.  $R \sim 750$ ) does not affect the  $^{12}\text{CO}(2-0)$  vs.  $T_{\text{eff}}$  relation. This also indicates that the CO index is insensitive to spectral resolution and could therefore be used more generally.

Figure 3 shows a similar plot but using the  $^{12}\text{CO}(3-1)$  band centered at  $\lambda_c = 2.3245 \mu\text{m}$ . We use the same continuum points as for the  $^{12}\text{CO}(2-0)$  band (see Table. 1). We see here again a very tight relation between  $T_{\text{eff}}$  and the  $^{12}\text{CO}(3-1)$  band. A linear least square fit gives us this relation with  $T_{\text{eff}} = 4974.85 - 56.53 \times \text{CO}(3-1)$  with an r.m.s of 120 K which is slightly higher as for  $^{12}\text{CO}(2-0)$ . However, both CO band heads are clearly excellent temperature indicators. In addition, we tried to measure the  $^{12}\text{CO}(4-2)$  band centered at  $\lambda_c = 2.3535 \mu\text{m}$ . Although we see clearly, as for the other bands, an increase of the band strength with decreasing temperature, the intrinsic scatter is much higher ( $\sim 200 \text{ K}$ ). For that reason we do not discuss further this relation.

How does the spectroscopic temperatures compare with those derived from photometric measurements?

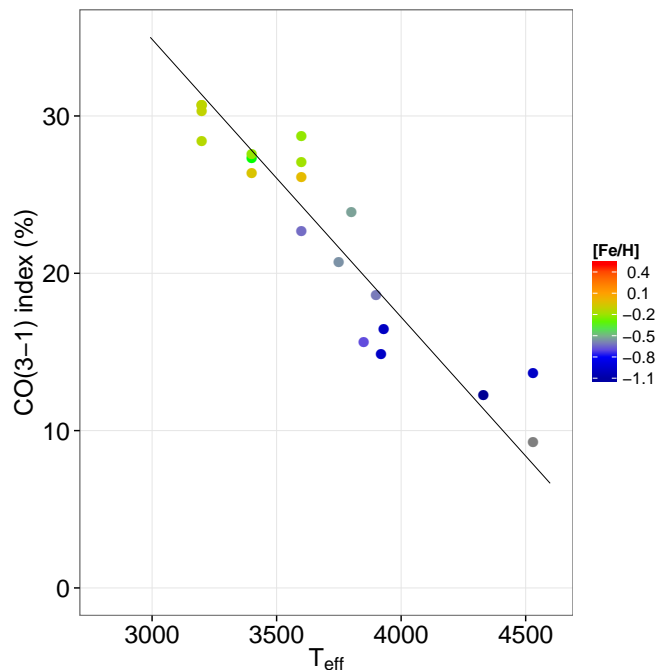


**Fig. 3.** Effective temperature vs.  $^{12}\text{CO}(3-1)$  band as a function of metallicity. The straight line shows our best fit.

Figure 4 shows the comparison between temperatures derived from photometric colours and from spectroscopy for our sample (see Table. 1) In order to calculate the photometric temperatures, we used here the temperature scale of M giants from Montegriffo et al. (1998) which is derived from black-body fits of population II stars and that of Houdashelt et al. (2000) using synthetic colors of M giants from MARCS models. We used the dereddened  $(J - K)_0$  colour of our stars to obtain the photometric temperatures. The mean difference between Montegriffo et al. (1998) and the temperatures from the  $^{12}\text{CO}(2-0)$  index is  $10 \text{ K} \pm 200$  while for the photometric temperatures of Houdashelt et al. (2000) they are about 90 K systematically higher with a higher r.m.s dispersion  $\pm 250 \text{ K}$ .

### 3.2. Metallicity

With the upcoming low-resolution multi-fiber near-IR spectrographs (MOONS, MOS, etc.), the main question arises how accurate one can get metallicities with low-resolution infrared spectra compared to high-resolution IR spectra. During the last years several studies came out to trace metallicity distribution functions as well as metallicity gradients. Gonzalez et al. (2011b) derived photometric metallicities based on VVV data along the bulge minor axis, where accurate high-resolution spectroscopic metallicities are available. They found a remarkable agreement between both methods. Gonzalez et al. (2013) obtained a full low-resolution metallicity map over the VVV Bulge footprint where they revealed a clear metallicity gradient of 0.28 dex/kpc. Due to the high extinction, this map is restricted to  $|b| > 3^\circ$ . Ramirez et al. (1997) have established an  $[\text{Fe}/\text{H}]$  scale for Galactic globular clusters based on medium-resolution (1500–3000) infrared K-band spectra. The technique uses the same absorption features we use here: NaI, Ca, and CO and was calibrated on globular cluster stars. The technique was calibrated and tested for globular cluster giants with  $-1.8 < [\text{Fe}/\text{H}] < -0.1$  and  $-7 < M_K < -4$  and has a typical uncertainty of  $\pm 0.1 \text{ dex}$ .

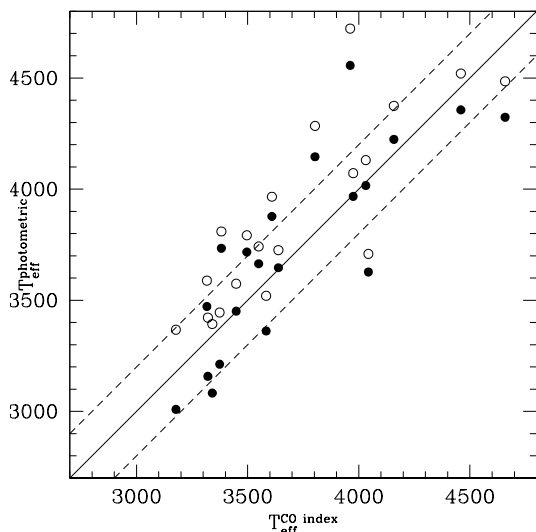


**Fig. 4.** Photometric temperatures vs. spectroscopically derived temperatures. Open circles use the relation by Houdashelt et al. (2000), black circles those from Montegriffo et al. (1998).

Ramírez et al. (2000) calculated metallicities for 110 M giants in the Inner Bulge using these spectral indices of NaI, Ca and CO. Schultheis et al. (2003) applied this technique to get the metallicity distribution of ISOGAL sources in the inner degree of our Galaxy. Do et al. (2015) observed low-resolution K-band spectra ( $R \sim 5000$ ) of late-type giants within the central 1 pc and obtained metallicities by fitting very sparsely sampled synthetic spectra, intended for calculating MARCS model atmospheres (which should actually not be used as synthetic stellar spectra; see the MARCS homepage; [www.marcs.astro.uu.se](http://www.marcs.astro.uu.se)). Their estimated uncertainties are consequently large, larger than 0.3 dex, with some very uncertain systematic effects leading to extremely metal-rich stars.

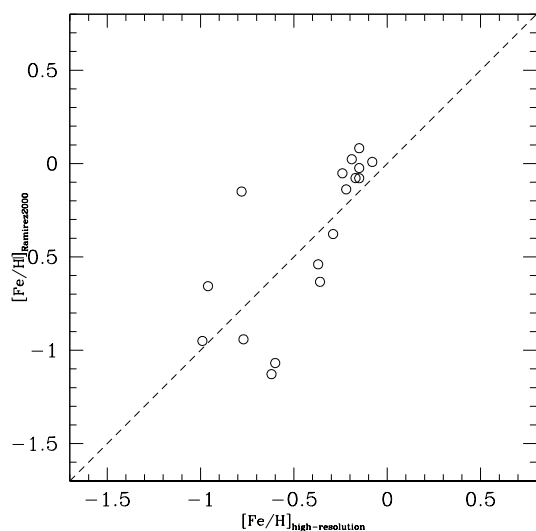


**Fig. 5.** [Fe/H] comparison between low-resolution spectra (Ramirez et al. 2000) and high resolution spectra from our calibration sample (Table 1).

We used solution 1 from Ramírez et al. (2000) which does not take any photometric quantities into account with the following relation:

$$[\text{Fe}/\text{H}] = -1.782 + 0.352 \times \text{EW}(\text{Na}) - 0.0231 \times \text{EW}(\text{Na})^2 - 0.0267 \times \text{EW}(\text{Ca}) + 0.0129 \times \text{EW}(\text{Ca})^2 + 0.0472 \times \text{EW}(\text{CO}) - 0.00109 \times \text{EW}(\text{CO})^2$$

where  $\text{EW}(\text{CO})$ ,  $\text{EW}(\text{Na})$  and  $\text{EW}(\text{Ca})$  are the equivalent widths of CO, Na and Ca, respectively. Figure 5 shows the comparison of metallicities derived as in Ramírez et al. (2000) from low-resolution spectra and those from high-resolution infrared spectra coming from our calibration sample. One can notice that there is a general correlation between the metallicities derived from high-resolution IR spectra and those from low-resolution spectra. The dispersion is in the order of  $\sim 0.2$  dex.

## 4. Application of the method to M giants in the galactic Bulge

### 4.1. Temperature

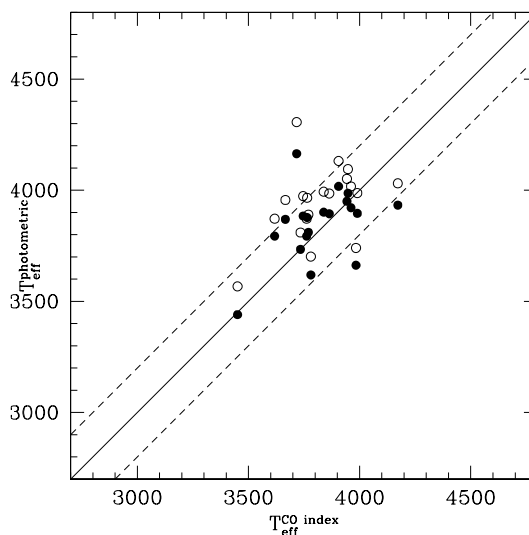


**Fig. 6.** Photometric temperatures vs. spectroscopically derived temperatures for the stars of Ryde et al. (2016). Open circles use the relation by Houdashelt et al. (2000), black circles those from Montegriffo et al. (1998). Due to the missing J counterpart, the stars in the galactic Center (see Table 2) were omitted.

We applied this method to the M giants sample of Ryde et al. (2016) located in the inner 300 pc of the Milky Way. Figure 6 shows the comparison between our method and photometrically derived temperatures. We see here a more scattered diagram which is due to variable, patchy extinction making the photometric temperatures less reliable. Due to the extreme high extinction in the galactic Center region, the M giants of Ryde & Schultheis (2015) do not have J counterparts and are not included in Fig. 6

### 4.2. Metallicity

Figure 7 shows the application of this method to the M giant Bulge sample of Ryde & Schultheis (2015) and Ryde et al. (2016). We see an increased spread or even a plateau at about  $[\text{Fe}/\text{H}] = 0.0$  for the low-resolution part where the metal-rich stars do not follow this relation anymore. This indicates that the Na and the Ca lines saturate in the most metal-rich stars. Indeed,

by tracing the equivalent width of NaI and CaI alone, one see this plateau at around solar metallicity. This means that the proposed relation of Ramírez et al. (2000) is only valid for M giants with sub-solar metallicities. Therefore this metallicity index is not suited for galactic Bulge studies or at least for the metal-rich component of the metallicity distribution of bulge stars but can be used in low-metallicity systems such as globular clusters or dwarf spheroidals.

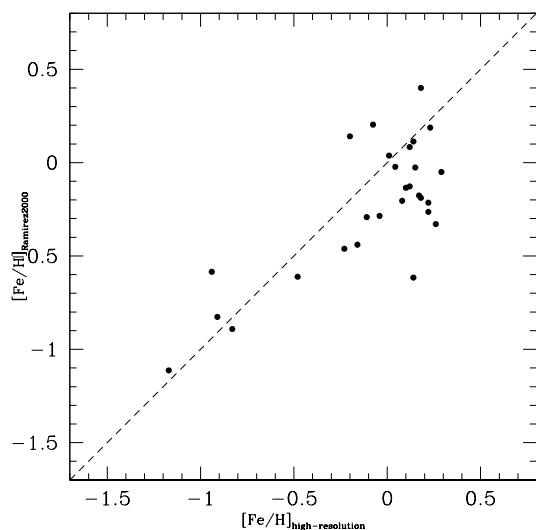


**Fig. 7.** [Fe/H] comparison between low-resolution spectra and high resolution spectra for the stars from Ryde & Schultheis (2015) and Ryde et al. (2016).

## 5. Conclusions

In high extinguished regions such as the galactic Bulge and especially the galactic Center, the precision in the photometric temperatures and gravities are hampered by the poor knowledge of interstellar extinction. We have studied 20 well-known M giants with well-known stellar parameters and covering the temperature range  $3200 < T_{\text{eff}} < 4500$  K and with a metallicity range  $-1.2 < [\text{Fe}/\text{H}] < 0.5$ . We confirm the straight relation found by Blum et al. (2003) between  $T_{\text{eff}}$  and the  $^{12}\text{CO}(2-0)$  index with a dispersion of 95 K. We also find a relation between  $^{12}\text{CO}(3-1)$  and  $T_{\text{eff}}$  with a dispersion of 120 K. We do not find any critical dependence of these relations on metallicity or on the adopted spectral resolution, which makes them a very powerful tool to obtain accurate temperatures in the Inner galactic Bulge and the galactic Center which has been applied by Ryde & Schultheis (2015) and Ryde et al. (2016). Finally, we confirm that the combination of NaI, CaI and CO band is an excellent metallicity index as pointed out by Ramírez et al. (2000). However, this relation is only valid for M giants with sub-solar metallicities but can not be applied for metal-rich stars and thus for the metal-rich part of the galactic Bulge.

*Acknowledgements.* We want to thank the referee L. Origlia for her extremely useful comments and suggestions. N.R. acknowledges support from the Swedish Research Council, VR (project number 621-2014-5640), and Funds from Kungl. Fysiografiska Sällskapet i Lund. (Stiftelsen Walter Gyllenbergs fond and Märta och Erik Holmbergs donation).

## References

- Blum, R. D., Ramírez, S. V., Sellgren, K., & Olsen, K. 2003, ApJ, 597, 323  
 Do, T., Kerzendorf, W., Winsor, N., et al. 2015, ApJ, 809, 143  
 Frogel, J. A., Stephens, A., Ramírez, S., & DePoy, D. L. 2001, AJ, 122, 1896  
 Gonzalez, O. A., Rejkuba, M., Zoccali, M., et al. 2011a, A&A, 530, A54  
 Gonzalez, O. A., Rejkuba, M., Zoccali, M., et al. 2013, A&A, 552, A110  
 Gonzalez, O. A., Rejkuba, M., Zoccali, M., Valenti, E., & Minniti, D. 2011b, A&A, 534, A3  
 Gonzalez, O. A., Rejkuba, M., Zoccali, M., et al. 2012, A&A, 543, A13  
 González Hernández, J. I. & Bonifacio, P. 2009, A&A, 497, 497  
 Houdashelt, M. L., Bell, R. A., & Sweigart, A. V. 2000, AJ, 119, 1448  
 Ivanov, V. D., Rieke, M. J., Engelbracht, C. W., et al. 2004, ApJS, 151, 387  
 Monaco, L., Villanova, S., Moni Bidin, C., et al. 2011, A&A, 529, A90  
 Montegriffo, P., Ferraro, F. R., Origlia, L., & Fusi Pecci, F. 1998, MNRAS, 297, 872  
 Pfuhl, O., Fritz, T. K., Zilka, M., et al. 2011, ApJ, 741, 108  
 Ramirez, S. V., Depoy, D. L., Frogel, J. A., Sellgren, K., & Blum, R. D. 1997, AJ, 113, 1411  
 Ramírez, S. V., Stephens, A. W., Frogel, J. A., & DePoy, D. L. 2000, AJ, 120, 833  
 Rich, R. M. & Origlia, L. 2005, ApJ, 634, 1293  
 Rich, R. M., Origlia, L., & Valenti, E. 2012, ApJ, 746, 59  
 Ryde, N. & Schultheis, M. 2015, A&A, 573, A14  
 Ryde, N., Schultheis, M., Grieco, V., et al. 2016, AJ, 151, 1  
 Schultheis, M., Chen, B. Q., Jiang, B. W., et al. 2014, A&A, 566, A120  
 Schultheis, M., Ganesh, S., Simon, G., et al. 1999, A&A, 349, L69  
 Schultheis, M., Lançon, A., Omont, A., Schuller, F., & Ojha, D. K. 2003, A&A, 405, 531  
 Schultheis, M., Sellgren, K., Ramírez, S., et al. 2009, A&A, 495, 157